

Support-Area Dependence of Vibration-Insensitive Optical Cavities

Won-Kyu Lee^{1,2,*}, Sang Eon Park^{1,2}, Chang Yong Park^{1,2},
Dai-Hyuk Yu¹, Myoung-Sun Heo¹, and Huidong Kim¹

¹Korea Research Institute of Standards and Science, Daejeon 34113, Korea

²University of Science and Technology, Yuseong, Daejeon 34113, Korea

*Corresponding author: oneqlee@kriss.re.kr

The vibration sensitivities of optical cavities depending on the support-area were investigated both numerically and experimentally. We performed the numerical simulation with two models; one with total constraint over the support area, and the other with only vertical constraint. A support-area-size insensitive optimal support condition could be found by the numerical simulation. The support-area was determined in the experiment by a Viton rubber pad. The vertical, transverse, and longitudinal vibration sensitivities were measured experimentally. The experimental result agreed with the numerical simulation with a sliding model (only vertical constraint).

I. INTRODUCTION

Narrow linewidth lasers are essential tools for various applications including optical clocks [1-4], low-phase-noise microwave generation [5], fundamental tests of relativity [6], gravitational wave detection [7], and dark matter search [8]. The laser linewidth is narrowed usually by stabilizing its frequency onto an ultra-stable optical cavity resonance. Because this optical cavity is sensitive to external vibration noises, there have been a number of researches during the last decade on the support methods to minimize its sensitivity for both horizontal cavities [9-13] and vertical ones [14, 15], and the laser frequency stability reached the thermal noise limit which is given by Brownian noise from mirror coatings, mirror substrates, and cavity spacers [11, 15]. To decrease the thermal noise limit further [16], researches are being actively undertaken with longer cavities [16-20], with cavities at cryogenic temperatures [21, 22], or using new material with lower mechanical loss [23]. However, longer cavities are generally more sensitive to the vibration noise, and their frequency stabilities are still limited by seismic noise [20]. Thus, more works are required in reducing the vibration sensitivity of optical cavities.

For the clock lasers of the Yb optical lattice clock at KRISS (Korea Research Institute of Standards and Science) [24-26], cut-out-type vibration-insensitive horizontal optical cavities were adopted [10, 11]. Optimal cavity support positions with smallest vibrational sensitivity can be determined by numerical simulations before the experiments [9-23]. Optical cavities are usually supported by small Viton rubber balls [10, 11, 17, 18, 20], however, considering that the rubber balls can be squeezed, the numerical simulations have limitations in this case because the support area sizes are ambiguous and the pressure distribution over the support area is not uniform. With this concern, we used Viton pads instead of balls to support the optical cavity. We performed finite element analysis (FEA) for the vibrational sensitivity of our cavities varying the support positions and the support area diameter with the fixed support point condition (fully constrained) and the sliding support condition (only vertically constrained). Also, a support-area-size insensitive optimal support condition could be found. We compared these numerical simulations with the experimental results.

II. CAVITY DESIGN AND FINITE ELEMENT ANALYSIS

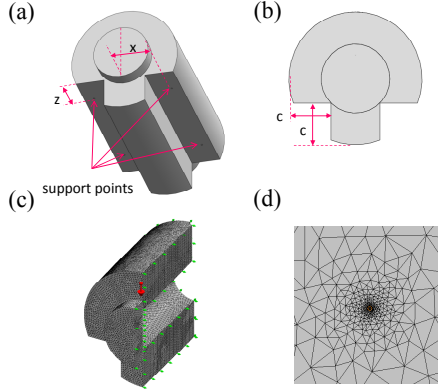


Figure 1. (a) Positions of the four support points with the transverse displacement of x and the longitudinal displacement of z , (b) Front view of the cavity with the cut-out depth of c , (c) Numerical simulation of the cavity deformation, (d) Meshes in the finite element analysis around a support point.

The shape of the cavity in this research is shown in Fig. 1(a) and Fig. 1(b) with the definition of the cut-out depth c . We used two cavities with the only difference of the cut-out depth; 18.45 mm for Cavity1 and 19.45 mm for Cavity2. The positions of the support points are shown in Fig. 1(a) with the transverse displacement of x and the longitudinal displacement of z . The length and the outer diameter of the cavity spacer are 100 mm and 60 mm, respectively. The spacer has a bore with a diameter of 12.5 mm, and has a vertical vent-hole in the middle with a diameter of 4 mm. The cavity is formed with a plane mirror and a concave mirror with a radius of curvature of 500 mm. The diameter and the thickness of the mirrors are 25.4 mm and 6.2 mm, respectively. The cavity spacer and the mirror substrates are made of ultra-low-expansion glass (ULE® [27]). With multilayer dielectric coating, the finesse values were 160,000 and 300,000 for Cavity1 and Cavity2, respectively, at 578 nm. The mirror substrates have anti-reflective coatings at outer surfaces.

The locations of the support points have to be optimized to minimize the vibration sensitivities [9-23]. Thus, we performed finite element analysis (FEA) to estimate the optimal positions of support points by varying c , x and z [28]. We simulated with only a quarter section of the cavity (Fig. 1(c)) to reduce computation time considering the symmetry. We also performed FEA with various diameter d of the support point. The areas of the support points were defined by those of the Viton pads in our experiment. Two kinds of simulation model were adopted; one with the fixed

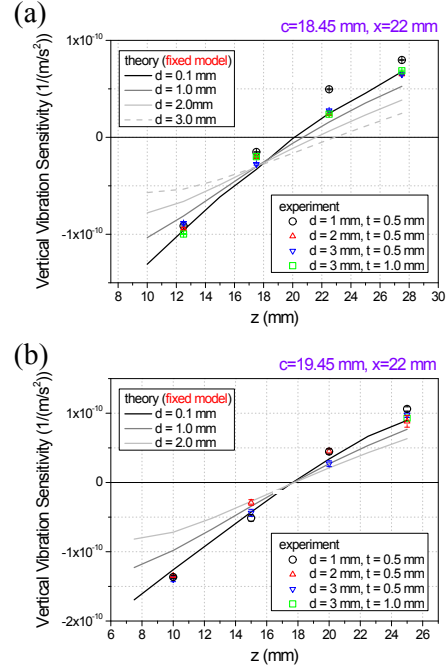


Figure 2. (a) Dependence of the vertical vibration sensitivity of Cavity1 on z and on the size of the support point diameter d , which was calculated by the FEA with fixed supports. The values of c and x were fixed to 18.45 mm and 22 mm, respectively. The experimentally measured values are also plotted with various support diameter and thickness, (b) The dependence of Cavity2 with the same condition as in (a) except for the change of the value of c to 19.45 mm.

model (the support areas were totally fixed) and the other with the sliding model (the support areas were only vertically fixed). The material parameters of ULE used in the FEA were the Poisson's ratio of 0.17, the density of 2.21 g/cm³, and the elastic modulus of 67.6 GPa [27]. Typical meshes in the FEA are shown in Fig. 1(d), whose maximum sizes were 0.1 mm for the support areas and on the high-reflective-coated mirror surfaces, and 1 mm for other parts of the cavity. The FEA was done statically because the seismic noise with higher frequency would be attenuated by vibration isolators in the experiment. The change of the cavity length was obtained by calculating the distance between the center points of the two mirror surfaces when static vertical acceleration of 1 g (9.8 m/s²) was applied.

In Fig. 2(a), the FEA result for Cavity1 with the fixed model is shown by varying d and z . The vibration sensitivity (the normalized change of the cavity length divided by the acceleration) depending on z is shown with the d values of 0.1 mm, 1.0 mm,

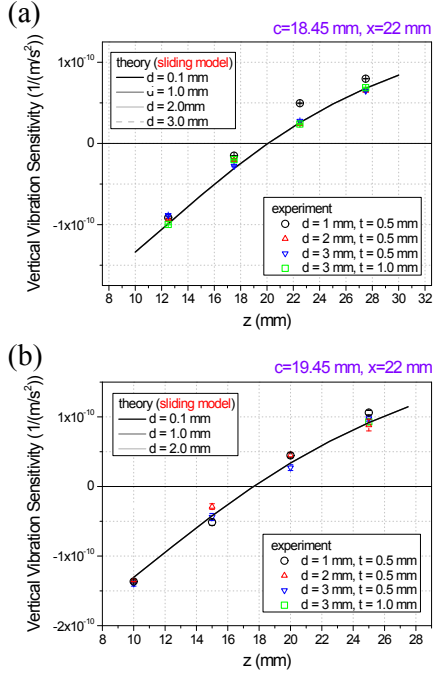


Figure 3. (a) Dependence of the vertical vibration sensitivity of Cavity1 calculated by the FEA with sliding supports. The values of c and x were fixed to 18.45 mm and 22 mm, respectively. The experimentally measured values are also plotted with various support diameter and thickness, (b) The dependence of Cavity2 with the same condition as in (a) except for the change of the value of c to 19.45 mm.

2.0 mm, and 3.0 mm. The values of c and x were fixed to 18.45 mm and 22 mm, respectively. We found that z positions for zero longitudinal displacement (i.e. minimum vibration sensitivity) are different for various support areas. There exists only one set of parameters giving minimum vibration sensitivity for various diameters of support area. We also found a c -value for which the z values for the minimum vibration sensitivity are the same regardless of the support area by the FEA. When the value of c was changed to 19.45 mm with the same value of the other parameters, a support-area-size independent support condition was found at $z = 17.5$ mm as in Fig. 2(b), on the basis of which Cavity2 was designed. As stated in the introduction, when a rubber balls are used for the cavity support, there is ambiguity for the support area. This support-area-size independent condition is expected to be useful in this situation. It is notable that the smaller the support area, the larger the slope (the vibration sensitivity per longitudinal displacement) for both Cavity1 and Cavity2.

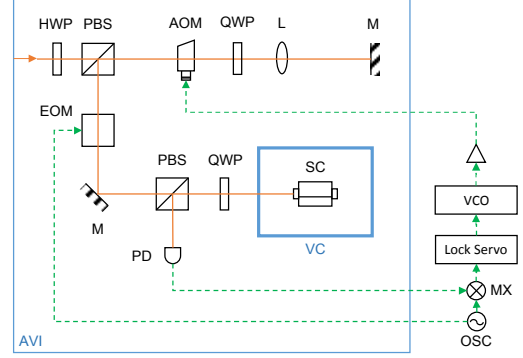


Figure 4. Experimental setup for the vibration sensitivity measurement. AVI, active vibration isolator; HWP, half-wave plate; PBS, polarizing beam splitter; AOM, acousto-optic modulator; L, lens; M, mirror; EOM, electro-optic modulator; QWP, quarter-wave plate; PD, photo-diode; SC, super-cavity; VC, vacuum chamber; VCO, voltage controlled oscillator, MX, mixer, OSC, two-channel function generator.

The dependence of the vertical vibration sensitivity of Cavity1 and Cavity2 calculated by the FEA with sliding model is shown in Fig. 3(a) and Fig.3(b), respectively. In this case, there was no dependence of the vibrational sensitivity on the support-area-size, and the z -dependence was approximately the same as that of very small support-area with fixed model ($d = 0.1$ mm in Fig. 2). This result seems reasonable because sliding model can be considered to be the small area limit of the fixed model. The z values for zero longitudinal displacement were 20.0 mm and 17.5 mm for Cavity1 and Cavity2, respectively.

III. EXPERIMENTAL SETUP

Figure 4 shows the experimental setup for the vibration sensitivity measurement. The laser has wavelength of 578 nm [25, 29, 30], which is a probe laser for Yb lattice clock transition. The frequency of the input laser in Fig. 4 was stabilized in advance to a resonance of another cavity which has the same design as Cavity2 by the Pound-Drever-Hall (PDH) method [31]. The frequency of the input laser beam is shifted by a double pass AOM (acousto-optic modulator) which is driven by a VCO (voltage controlled oscillator), thus, it can be considered to be an independent laser source compared with the original input. And then we used a PDH setup to stabilize the laser frequency to a resonance of either Cavity1 or Cavity2, as in Fig. 4. The optical cavity was contained in a vacuum chamber. The PDH error signal was fed back to the VCO for the stabilization. The frequency

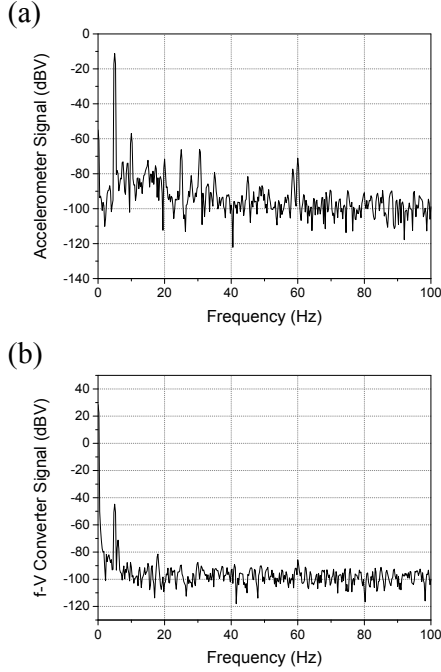


Figure 5. Synchronous measurement of (a) the signal of the accelerometer, (b) and the signal of the f-V converter by using a spectrum analyzer.

change by the vibration was measured by the beat note between this stabilized laser and the original input laser. The frequency of this beat note signal was converted into a voltage signal using a frequency-to-voltage converter. The vacuum chamber and the optical setup were placed on an active vibration isolation table (AVI) (TS-300/LP, The TableStable Ltd.). The AVI was used in a “shaker” mode to provide a sinusoidal acceleration in one of the three orthogonal direction to measure the vibration sensitivity. The magnitude of the acceleration was measured by a three-axis accelerometer. The frequency of the sinusoidal acceleration was chosen to be 5 Hz, in a condition that the cavity deformation could be considered to be quasi-static and the cross-coupling among the vertical acceleration and two horizontal (transverse and longitudinal) accelerations was suppressed by more than 20 dB. The magnitude of the acceleration and the frequency-to-voltage converter was measured simultaneously by using a spectrum analyzer and by measuring the signals at 5 Hz (Figure 5). The cavity was supported with four Viton pads (Fig. 6(a), (b)). The Viton pads with various diameters between 1 mm and 5 mm were made using hole punches and 0.5-mm-thick Viton sheets. The picture of the produced Viton pad is shown in Fig. 6(d).

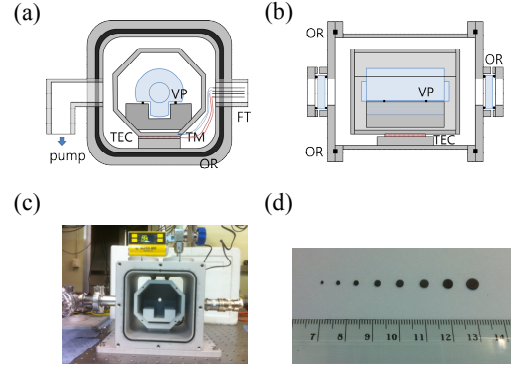


Figure 6. (a) Front view of the vacuum chamber for the vibration sensitivity measurement. TEC, thermoelectric cooler; TM, thermistor; FT, 4-pin feed-through; VP, Viton pad; OR, O-ring seal, (b) Side view of the vacuum chamber, (c) Picture of the cavity installed in the partly assembled vacuum chamber, (d) Picture of the Viton support pads produced by hole-punches.

Since we have to open the vacuum chamber frequently to measure the vibration sensitivity at various support points with many kinds of Viton pads, the vacuum chamber covers were sealed with o-rings (Fig. 6(a), (b)). The vacuum chamber was made of aluminum for convenient temperature control (by a thermoelectric cooler and a thermistor), which would have advantages in finding the temperature for zero thermal expansion coefficient of the ULE cavity. The size of the vacuum chamber was 188 mm x 188 mm x 204 mm. The windows have anti-reflection coatings at 578 nm. The picture of the vacuum chamber with a cavity is given in Fig. 6(c).

IV. RESULTS

The experimental result of the vibration sensitivity of vertical acceleration for Cavity1 and Cavity2 is shown in Fig. 2(a) and Fig. 2(b), respectively, together with the result of the numerical simulation by the fixed model. The frequency change was normalized with the optical frequency. Four kinds of the Viton pads were used in the experiment with various diameters and thicknesses. The vibrational sensitivities were measured at four z-positions for each cavity. Each of the vibrational sensitivities was obtained by averaging ten measurements, and the error bars represent the standard deviations. As can be seen in Fig. 2, the experimental results agrees well with the numerical simulation with small fixed support area. This experimental result is also shown with the result of the numerical simulation with the sliding model in Fig. 3,

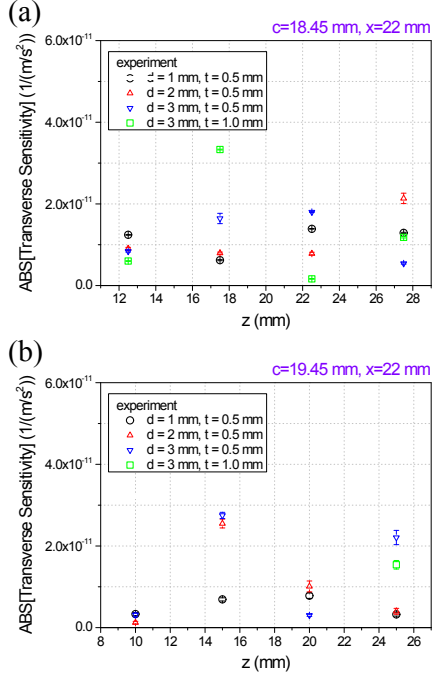


Figure 7. (a) Experimentally measured values of the transverse vibration sensitivity with various support diameter and thickness. c and x were fixed to 18.45 mm and 22 mm, respectively. (b) The same dependence as in (a), when only the value of c was changed to 19.45 mm.

and they agreed well with each other. This result can be interpreted that the sliding model seems to be more appropriate considering that the Viton rubber material can be deformed easily because it is mechanically soft. If we assume that the experimental uncertainty of 0.5 mm in locating the z -position for the zero vertical vibration sensitivity, it can be concluded that the vertical vibration sensitivities are less than $7 \times 10^{-12}/(\text{m/s}^2)$ and $9 \times 10^{-12}/(\text{m/s}^2)$, respectively for Cavity1 and Cavity2.

We also measured the horizontal (transverse and longitudinal) vibration sensitivities for both cavities. We could measure only the magnitude of the horizontal vibration sensitivities, because the small signal of the frequency change made it difficult to determine the sign. The vibration sensitivity measurement result for the acceleration in transverse direction is shown in Fig. 7, and most of the values were less than $2 \times 10^{-11}/(\text{m/s}^2)$ for both cavities. The vibration sensitivity measurement result for the acceleration in longitudinal direction is shown in Fig. 8. The distribution of the longitudinal vibration sensitivity values were more scattered, however, they were mostly less than $5 \times 10^{-11}/(\text{m/s}^2)$.

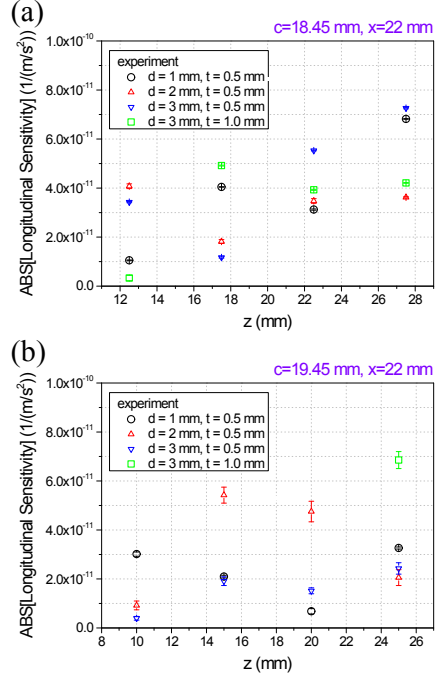


Figure 8. (a) Experimentally measured values of the longitudinal vibration sensitivity with various support diameter and thickness. c and x were fixed to 18.45 mm and 22 mm, respectively. (b) The same dependence as in (a), when only the value of c was changed to 19.45 mm.

To explain the scattering of the vibration sensitivities, we performed the repeatability test of the measurement. We obtained five vibration sensitivity values for each direction at the same condition (Fig. 9) but with new installations of the cavity. The vertical sensitivity had the average value of $2.9 \times 10^{-11}/(\text{m/s}^2)$ and the standard deviation of $5.9 \times 10^{-12}/(\text{m/s}^2)$. The transverse sensitivity had the average value of $1.2 \times 10^{-11}/(\text{m/s}^2)$ and the standard deviation of $1.0 \times 10^{-11}/(\text{m/s}^2)$. The longitudinal sensitivity had the average value of $3.1 \times 10^{-11}/(\text{m/s}^2)$ and the standard deviation of $1.8 \times 10^{-11}/(\text{m/s}^2)$. These results are consistent with the scattering of the vibration sensitivities in Fig. 2, Fig. 3, Fig. 7, and Fig. 8, thus it can be concluded that the scattering of the vibration sensitivity measurement was due to the experimental repeatability of the cavity support location.

V. CONCLUSION

We investigated the support-area dependence of vibration sensitivities of optical cavities by numerical simulations and by experiments. Following the numerical simulation result, a new cavity was designed which has a vibration-insensitive support position independent of the size of the support area. The numerical simulation was performed with two models; one with total constraint over the support area, and the other with only vertical constraint. The experimental result agreed well with the model with vertical constraint. The vibration sensitivities in three orthogonal directions (vertical, transverse, and

longitudinal directions) were measured. The scattering of the sensitivity measurement could be explained by the location repeatability of the cavity support.

REFERENCES

1. S. L. Campbell, R. B. Hutson, G. E. Marti, A. Goban, N. Darkwah Oppong, R. L. McNally, L. Sonderhouse, J. M. Robinson, W. Zhang, B. J. Bloom, and J. Ye, "A Fermi-degenerate three-dimensional optical lattice clock," *Science* **358**, 90-94 (2017).
2. M. Schioppo, R. C. Brown, W. F. McGrew, N. Hinkley, R. J. Fasano, K. Beloy, T. H. Yoon, G. Milani, D. Nicolodi, J. A. Sherman, N. B. Phillips, C. W. Oates, and A. D. Ludlow, "Ultrastable optical clock with two cold-atom ensembles," *Nat. Photonics* **11**, 48-52 (2017).
3. N. Nemitz, T. Ohkubo, M. Takamoto, I. Ushijima, M. Das, N. Ohmae, and H. Katori, "Frequency ratio of Yb and Sr clocks with 5×10^{-17} uncertainty at 150 seconds averaging time," *Nat. Photonics* **10**, 258-261 (2016).
4. H. Kim, M.-S. Heo, W.-K. Lee, C. Y. Park, H.-G. Hong, S.-W. Hwang, and D.-H. Yu, "Improved absolute frequency measurement of the ^{171}Yb optical lattice clock at KRISS relative to the SI second," *Jpn. J. Appl. Phys.* **56**, 050302 (2017).
5. A. Bartels, S. A. Diddams, C. W. Oates, G. Wilpers, J. C. Bergquist, W. H. Oskay, and L. Hollberg, "Femtosecond-laser-based synthesis of ultrastable microwave signals from optical frequency references," *Opt. Lett.* **60**, 667-669 (2005).
6. E. Wiens, A. Yu. Nevsky, and S. Schiller, "Resonator with ultrahigh length stability as a probe for equivalence-principle-violating physics," *Phys. Rev. Lett.* **117**, 271102 (2016).
7. S. Kolkowitz, I. Pikovski, N. Langellier, M. D. Lukin, R. L. Walsworth, and J. Ye, "Gravitational wave detection with optical lattice atomic clocks," *Phys. Rev. D* **94**, 124043 (2016).
8. A. A. Geraci, C. Bradley, D. Gao, J. Weinstein, and A. Derevianko, "Searching for ultra-light dark matter with optical cavities," *arXiv1808.00540* (2018).
9. J. Millo, D. V. Magalhães, C. Mandache, Y. Le Coq, E. M. L. English, P. G. Westergaard, J. Lodewyck, S. Bize, P. Lemonde, and G. Santarelli, "Ultrastable lasers based on vibration insensitive cavities," *Phys. Rev. A* **79**, 053829 (2009).

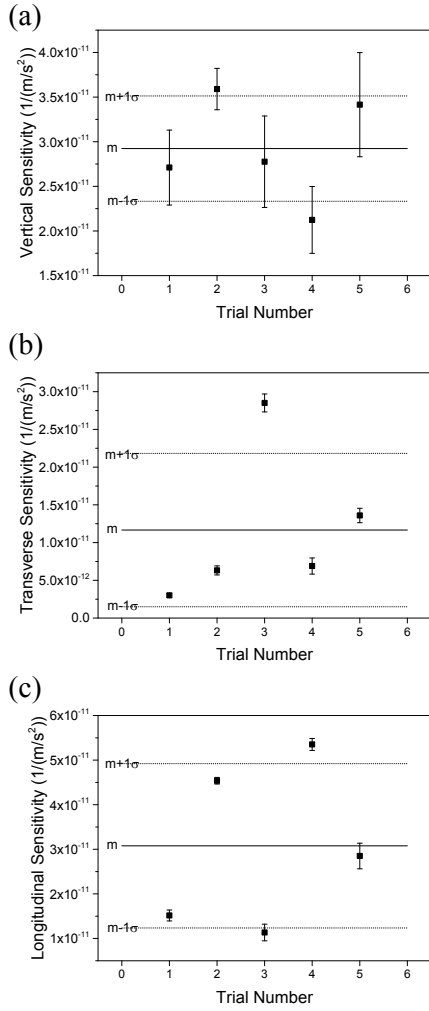


Figure 9. Repeatability of the measurement of the vibration sensitivity. Solid line and the dotted lines indicate the value of the mean (m) and the standard deviation (σ) for five measurements. (a) Vertical sensitivity; $m=2.9 \times 10^{-11}$, $\sigma=5.9 \times 10^{-12}$, (b) Transverse sensitivity; $m=1.2 \times 10^{-11}$, $\sigma=1.0 \times 10^{-11}$, (c) longitudinal sensitivity; $m=3.1 \times 10^{-11}$, $\sigma=1.8 \times 10^{-11}$.

10. S. A. Webster, M. Oxborrow, and P. Gill, "Vibration insensitive optical cavity," *Phys. Rev. A* **75**, 011801(R) (2007).
11. S. A. Webster, M. Oxborrow, S. Pugla, J. Millo, and P. Gill, "Thermal-noise-limited optical cavity," *Phys. Rev. A* **77**, 033847 (2008).
12. T. Nazarova, F. Riehle, and U. Sterr, "Vibration-insensitive reference cavity for an ultra-narrow-linewidth laser," *Appl. Phys. B* **83**, 531-536 (2006).
13. Y. N. Zhao, J. Zhang, A. Stejskal, T. Liu, V. Elman, Z. H. Lu, and L. J. Wang, "A vibration-insensitive optical cavity and absolute determination of its ultrahigh stability," *Opt. Express*, **17**, 8970-8982 (2009).
14. M. Notcutt, L.-S. Ma, J. Ye, and J. L. Hall, "Simple and compact 1-Hz laser system via an improved mounting configuration of a reference cavity," *Opt. Lett.* **30**, 1815-1817 (2005).
15. A. D. Ludlow, X. Huang, M. Notcutt, T. Zanon-Willette, S. M. Foreman, M. M. Boyd, S. Blatt, and J. Ye, "Compact, thermal-noise-limited optical cavity for diode laser stabilization at 1×10^{-15} ," *Opt. Lett.* **32**, 641 (2007).
16. S. Amairi, T. Legero, T. Kessler, U. Sterr, J. B. Wübbena, O. Mandel, P. O. Schmidt, "Reducing the effect of thermal noise in optical cavities," *Appl. Phys. B* **113**, 233-242 (2013).
17. J. Keller, S. Ignatovich, S. A. Webster, T. E. Mehlstäubler, "Simple vibration-insensitive cavity for laser stabilization at the 10^{-16} level," *Appl. Phys. B* **116**, 203-210 (2014).
18. Y. Y. Jiang, A. D. Ludlow, N. D. Lemke, R. W. Fox, J. A. Sherman, L.-S. Ma, and C. W. Oates, "Making optical atomic clocks more stable with 10^{-16} -level laser stabilization," *Nat. Photonics* **5**, 158-161 (2011).
19. T. L. Nicholson, M. J. Martin, J. R. Williams, B. J. Bloom, M. Bishof, M. D. Swallows, S. L. Campbell, and J. Ye, "Comparison of two independent Sr optical clocks with 1×10^{-17} stability at 10^3 s," *Phys. Rev. Lett.* **109**, 230801 (2012).
20. S. Häfner, S. Falke, C. Grebing, S. Vogt, T. Legero, M. Merimaa, C. Lisdat, and U. Sterr, " 8×10^{-17} fractional laser frequency instability with a long room-temperature cavity," *Opt. Lett.* **40**, 2112-2115 (2015).
21. T. Kessler, C. Hagemann, C. Grebing, T. Legero, U. Sterr, F. Riehle, M. J. Martin, L. Chen, and J. Ye, "A sub-40-mHz-linewidth laser based on a silicon single-crystal optical cavity," *Nat. Photonics* **6**, 687-692 (2012).
22. D. G. Matei, T. Legero, S. Häfner, C. Grebing, R. Weyrich, W. Zhang, L. Sonderhouse, J. M. Robinson, J. Ye, F. Riehle, and U. Sterr, "1.5 μ m lasers with sub-10 mHz linewidth," *Phys. Rev. Lett.* **118**, 263202 (2017).
23. G. D. Cole, W. Zhang, M. J. Martin, J. Ye, and M. Aspelmeyer, "Tenfold reduction of Brownian noise in high-reflectivity optical coatings," *Nat. Photonics* **7**, 644-650 (2013).
24. C. Y. Park, D.-H. Yu, W.-K. Lee, S. E. Park, E. B. Kim, S. K. Lee, J. W. Cho, T. H. Yoon, J. Mun, S. J. Park, T. Y. Kwon, and S.-B. Lee, "Absolute frequency measurement of 1S_0 ($F = 1/2$) – 3P_0 ($F = 1/2$) transition of ^{171}Yb atoms in a one-dimensional optical lattice at KRISS," *Metrologia* **50**, 119-128 (2013).
25. D.-H. Yu, C. Y. Park, W.-K. Lee, S. Lee, S. E. Park, J. Mun, S.-B. Lee, and T. Y. Kwon, "An Yb optical lattice clock: current status at KRISS," *J. Korean Phys. Soc.* **63**, 883-889 (2013).
26. S. Lee, C. Y. Park, W.-K. Lee, and D.-H. Yu, "Cancellation of collisional frequency shifts in optical lattice clocks with Rabi spectroscopy," *New J. Phys.* **18**, 033030 (2016).
27. <https://www.corning.com/worldwide/en/products/advanced-optics/product-materials/semiconductor-laser-optic-components/ultra-low-expansion-glass.html>
28. The finite element analysis was carried out using SOLIDWORKS.
29. E. B. Kim, W.-K. Lee, C. Y. Park, D.-H. Yu, and S. E. Park, "Narrow linewidth 578 nm light generation using frequency-doubling with a waveguide PPLN pumped by an optical injection-locked diode laser," *Opt. Express*, **18**, 10308-10314 (2010).
30. W.-K. Lee, C. Y. Park, D.-H. Yu, S. E. Park, S.-B. Lee, and T. Y. Kwon, "Generation of 578-nm yellow light over 10 mW by second harmonic generation of an 1156-nm external-cavity diode laser," *Opt. Express*, **19**, 17453-17461 (2011).
31. R.W.P. Drever, J.L. Hall, F.V. Kowalski, J. Hough, G.M. Ford, A.J. Munley, H. Ward, "Laser phase and frequency stabilization using an optical resonator," *Appl. Phys. B* **31**, 97-105 (1983).